

Terrain analysis of three small landslides using drone images and lidar data

Ali P. Babaki¹, Jennifer Clarke² & Dwayne D. Tannant¹

¹ University of British Columbia, Kelowna, BC, Canada

² Clarke Geoscience Ltd., Kelowna, BC, Canada



GeoCalgary
2022 October
2-5
Reflection on Resources

ABSTRACT

A hiking trail within a regional park in Kelowna, BC, was recently developed over the remnants of a small cut and fill excavation for a historic water irrigation flume. The trail runs along the steep face of a glaciofluvial terrace. In the spring of 2018, a short period of intense rainfall triggered three small landslides near the trail. These transformed into debris flows or flowslides that descended 80 m down a steep valley wall to the creek below. A study was conducted to understand the triggering mechanisms for these events. Aerial images captured with a drone and lidar data were used to map the area. Several profiles and cross-sections were extracted to analyze the terrain. The geometry, geology, surface and groundwater features and potential causes for each landslide are documented. One landslide was triggered by overland flow, while two landslides were likely initiated by high perched groundwater levels.

RÉSUMÉ

Un sentier de randonnée dans un parc régional à Kelowna, en Colombie-Britannique, a récemment été aménagé sur les vestiges d'une excavation pour un canal d'irrigation historique. Le sentier longe le versant escarpé d'une terrasse fluviale glacière. Au printemps 2018, une courte période de précipitations intenses a déclenché trois petits glissements de terrain près du sentier. Celles-ci se sont transformées en coulées de débris qui sont descendues 80 m le long d'un mur de vallée escarpé jusqu'au ruisseau en contrebas. Une étude a été menée pour comprendre ce qui est responsable de ces événements. Des images aériennes capturées avec un drone et des données lidar ont été utilisées pour cartographier la zone. Plusieurs profils et coupes ont été extraits pour analyser le terrain. La géométrie, la géologie, les caractéristiques des eaux de surface et des eaux souterraines et les causes potentielles de chaque glissement de terrain sont documentées. Un glissement de terrain a été déclenché par un écoulement de surface, tandis que deux glissements de terrain ont probablement été initiés par des niveaux d'eau souterraine de perches élevés.

1 INTRODUCTION

A hiking trail within a regional park in Kelowna, BC, was recently upgraded over the remnants of a small cut and fill excavation for a historic water irrigation flume. The irrigation flume was constructed in the 1920s to carry water to orchards in southeast Kelowna (Ruzesky and Carter, 1990). The former irrigation flume and current trail run along the steep face of a glaciofluvial terrace. The terrace is located above a steep bedrock-controlled valley. Figure 1 shows an orthophoto of the area.

In the spring of 2018, a short period of intense rainfall during the spring freshet triggered small landslides near the trail. The landslide debris flowed down to Mission Creek. The yellow dots in Figure 1 show the initiation locations for these events distributed along a 160 m length of the trail. A study was conducted to understand the cause and triggering mechanism for each landslide. Ongoing research is examining whether static liquefaction caused the west and middle landslides and if future events could occur.

A 2015 inspection of the old water flume trail identified small landslides and tension cracks in the fill material. Pre-2015 slope movements had deformed a roughly 10 m long section of the trail fill slope, involving the outer 1 to 2 m of the trail to a depth of approximately 1.5 m (approximate volume <math><20\text{ m}^3</math>). The deformation affected vegetation below the irrigation trail but did not extend downslope to Mission Creek. Adjacent to this landslide, a tension crack indicated that the soil fill beside the trail was unstable.

2 GEOLOGY AND TOPOGRAPHY

Bedrock in the general area is comprised of gneiss and granodiorite (Okulitch, 2013). The valley wall along the south side of Mission Creek at the study area is bedrock-controlled, with some exposures of gneiss.

Figure 2 shows a contour map of the area. The top of the terrace near the area of interest has an approximate elevation of 570 to 580 m, while Mission Creek is more than 100 m below at an elevation of ~469 m. The trail is located at approximately 551 m elevation.

The western part of the study area has a relatively uniform and steep slope from the crest of the terrace to the south bank of Mission Creek. The slopes range from 40° to 45°. These are relatively steep slopes in soils, yet the vegetated slope shows only minor evidence of deformation. The valley wall in the eastern part of the study area is less steep in the upper half and contains a few small incised gullies caused by surface runoff erosion. The lower part of the eastern slope contains very steep areas where bedrock is exposed. The transition from the steep lower slope to the less steep and gullied upper slope coincides with the bedrock contact.

Figure 3 shows a profile of the valley wall created from a lidar-based digital elevation model (DEM) along with the interpreted geology. The lower part of the valley wall is bedrock controlled, while a range of glacial sediments occurs on the upper part of the valley.

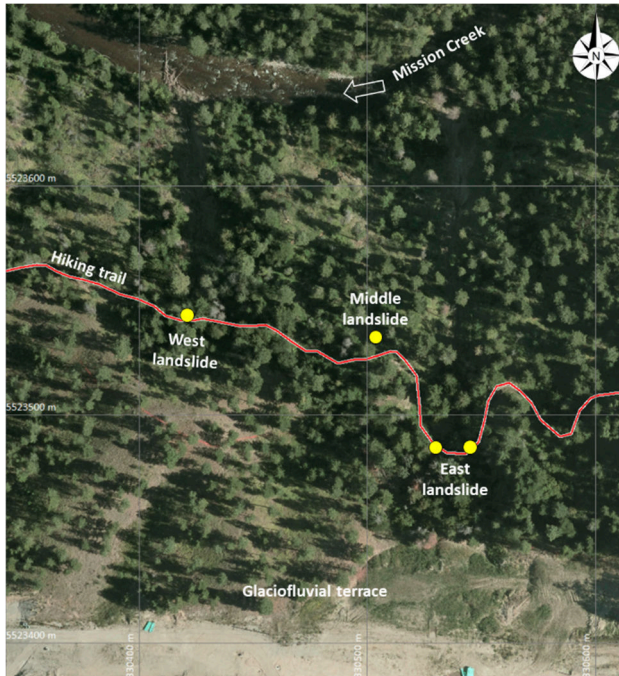


Figure 1. 2019 Orthophoto of the southern valley wall of Mission Creek showing the hiking trail in red and initiation locations for the landslides (100 m UTM grid)



Figure 2. Contour map (1 m interval) with drainage channels in blue and hiking trail in red

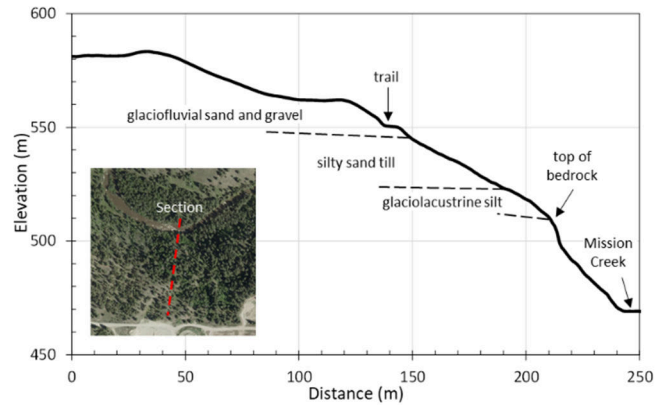


Figure 3. Cross-section showing interpreted geology

The surficial geology of the study area is reflective of the post-glacial history of the region over the past 10,000 years. When glacial ice was down-wasting and retreating from the highland plateau areas, ice occupied the lower Okanagan valley, resulting in the deposition of glaciolacustrine and glaciofluvial sediments along the flanks of Mission Creek. The upper sedimentary sequence was formed from meltwater fans and outwash terraces at the mouths of two tributary creeks to Mission Creek. The stratified sequence of sands and gravels transition to glaciolacustrine silts and glacial till (sandy silt with cobbles) lower down the slope. The glacial sediments are roughly 50 m thick and lie over bedrock. A thin mantle of colluvium and weathered soil in a loose state also covers the valley wall. Shallow test pits showed a significant increase in the soil density below a depth of 0.5 to 1 m. The thickness of the loose upper layer was increased locally by fill dumped down the slope during the irrigation trail construction. Beyond the slope crest, the glaciofluvial sand and gravel form an undulating raised terrace with hummocks and depressions. The sand and gravel sediments are relatively free-draining compared with the underlying silty sand till and glaciolacustrine silts.

3 SPRING 2018 WEATHER AND STREAMFLOW

A snow survey for April 1, 2018, reported a very high snowpack (201% of normal) at the McCulloch Snow Pillow (Stn. 2F03), located at the headwaters of Hydraulic Creek. In response to the spring freshet, Mission Creek experienced very high flows, with the 7-day average flows peaking during the week of May 10, 2018. Precipitation recorded at the Kelowna weather station (Env Can Stn. 1123939) recorded 22.1 mm on May 9, 2018. This was the highest daily precipitation for all of 2018. The Kelowna weather station rarely measures more than 20 mm of daily rainfall. ClimateBC reports annual mean precipitation of approximately 370 mm for the study area (ClimateBC, 2021).

The precipitation at the study location was likely higher than at the Kelowna weather station. The historical radar precipitation data collected at Silver Star Mountain (Historical Radar 2018) showed two intense bands of rainfall passed over the study area on May 9, 2018. Rainfall

intensities of up to 10 to 20 mm/hr were recorded from 01:00 to 05:00 and 06:30 to 09:00 PST.

4 VEGETATION AND GROUNDWATER

The study area occurs at a transition from a Ponderosa Pine to an Interior Douglas Fir biogeoclimatic zone (BC Ministry of Forests and Range, 2007). Figure 1 shows a variation in the tree density in the study area. Areas of denser growth may reflect possible groundwater pathways. It is postulated that perched water tables may occur above relatively low permeability layers of dense silt or dense silty till. The contact between the upper glaciofluvial sand and gravel and the lower glacial tills may constitute a region with groundwater seepage out of the valley wall during periods of precipitation and snowmelt. The old fill placed below the trail may have impeded groundwater seepage out of the slope.

5 DATA SOURCES AND FIELDWORK

The landslides are smaller than those typically investigated. Yet lidar and SfM data were still invaluable for estimating the landslide volumes and travel paths and classifying the landslide types.

The primary digital data sources were 2018 lidar data and a DEM derived from these data, and a set of 2020 aerial images acquired with a Remotely Piloted Aircraft System (drone). We used a DJI Phantom 4 Pro RTK and a DJI D-RTK 2 GNSS mobile base station to collect aerial images of the area on May 14, 2020. The collected GNSS data was post-processed to determine accurate camera coordinates for each image. A grid pattern was flown, and a series of oblique images were collected with a separate free flight. No ground control points were used.

The grid flights acquired 341 images with an approximate 80% forward and 75% side overlap of the flight lines. The drone was set to fly at a speed of 3.8 m/s to take photos nearly 12 m apart. For the grid flight, the camera elevation was held constant at 637 m. Figure 4 shows the flight path. Oblique images taken during a subsequent free flight captured the lower slope and debris flow paths.

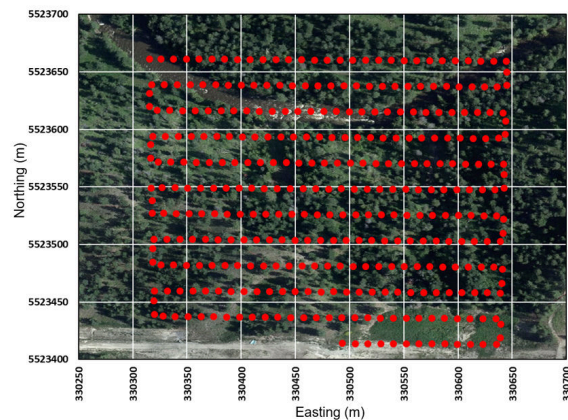


Figure 4. Drone flight path for capturing 341 images

A 2018 lidar point cloud and associated DEM dataset were obtained from the LidarBC data portal (LidarBC, 2021) by selecting the appropriate area of interest. A contour map of the area was generated from the DEM using GlobalMapper with a 1 m contour interval, as presented in Figure 2.

6 IMAGE AND POINT CLOUD PROCESSING

The GNSS observation file (rinex data) extracted from the drone was processed using the Natural Resources Canada Precise Point Positioning (PPP) tool (NRC 2022). In-house software and a custom-designed workflow were used to handle systematic formatting errors in the rinex file and to create a list of corrected UTM coordinates for the camera location for every image collected in the grid pattern.

The Canadian Spatial Reference System (NAD83) was used for the coordinate system. Both CGVD28 and CGVD2013 vertical reference systems were applied to process the images to confirm the datum used by the lidar data. The CGVD28 vertical datum was selected for the further process because it matched the lidar data shown in Figure 5. Obtaining the precise camera locations eliminated the need for ground control targets, although, for redundancy and precision checking, ground control should still be used.

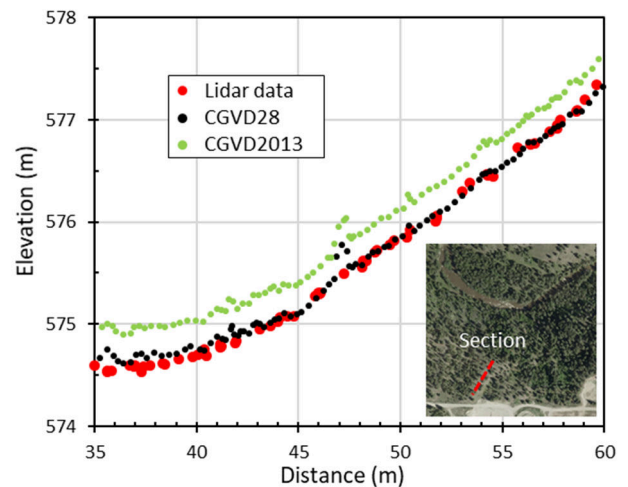


Figure 5. Two vertical datum systems (CGVD28 and CGVD2013) for image processing compared to available lidar data (5x vertical exaggeration)

We loaded the images and a list of their corrected UTM coordinates into the Structure-from-Motion (SfM) software Pix4D. The camera coordinates recorded in the EXIF header for each image were not used when processing the images. We used SfM software to generate a dense georeferenced 3D point cloud (Figure 6) and a georeferenced orthomosaic of the area.

Figure 7 shows a cross-section through point clouds generated by SfM and lidar techniques in a vegetated area. Although the density of points produced by SfM is higher, the line of sight to the ground surface is often blocked by

high vegetation (Asghar and Tannant, 2018). The lidar scanner had better penetration through the trees and captured more points on the ground surface.



Figure 6. Oblique view of a georeferenced 3D point cloud of the study area generated using the SfM technique

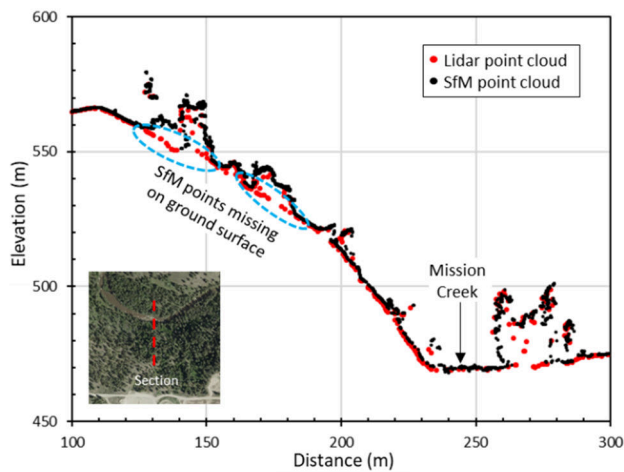


Figure 7. Cross-sections of SfM and lidar point clouds

Figure 8 shows a cross-section through DEMs produced from the lidar and SfM point clouds in a vegetated area. The lidar data was best at capturing the slope microtopography because more ground points were captured beneath the trees. The SfM-derived DEM missed some slope details, such as the hiking trail hidden by a dense tree canopy.

We used the orthomosaic and point cloud data (drone and lidar) to map each landslide's water drainage and debris path. Figure 9 shows three profile path locations in red overlaid on the SfM point cloud, and Figures 10 to 12 show the corresponding profiles.

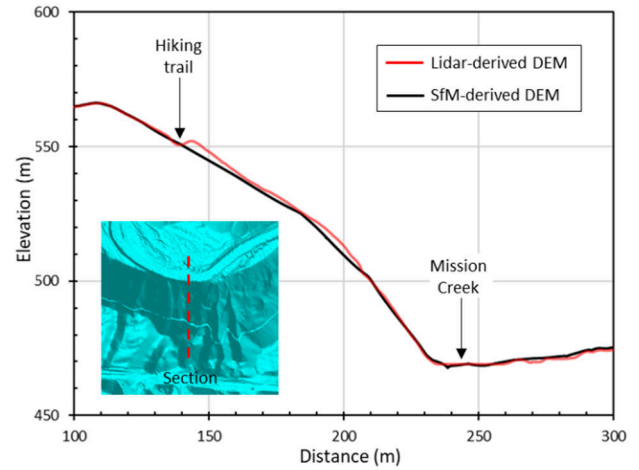


Figure 8. Cross-sections of DEMs generated from SfM and lidar point clouds

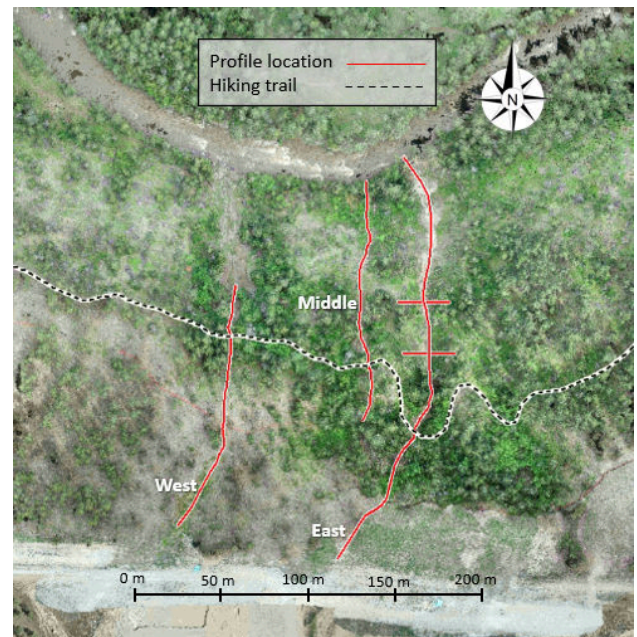


Figure 9. Plan view of SfM point cloud showing the profile lines for the west, middle and east landslides

7 WEST LANDSLIDE

The west landslide originated in an area of tension cracks along the outside edge of the trail. A profile through the slope and the landslide location is presented in Figure 10. The landslide initiated approximately 3 m below the trail on a steep ($\sim 42^\circ$) slope. Three mature trees are situated between the trail and the landslide headscarp and provide some stability to the trail due to root reinforcement. The near-vertical headscarp immediately north and below the trees is 3 to 4 m high. A perched water table above the lower permeability glacial till is believed to have been present when the landslide occurred, as shown in Figure 10.

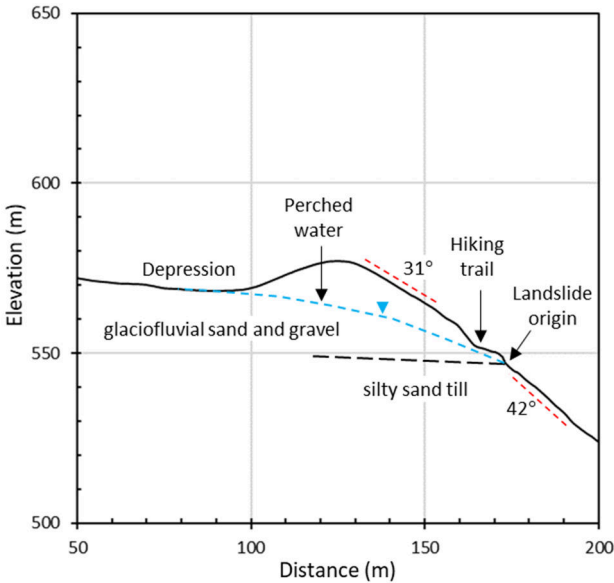


Figure 10. Slope profile for the west landslide

The landslide had an estimated source volume of 50 m³ and flowed approximately 120 m downslope, and deposited nearly 160 m³ of debris into Mission Creek. Debris entrainment along the travel path was approximately 110 m³. The landslide is classified as a flowslide (Hung et al., 2001; 2014) based on the source material (loose silty sand and fill), pore-water pressure generation, and the mobility of the landslide debris.

A small slump of soil at this location also occurred onto the trail. The slump deposited less than 10 m³ of soil onto the trail surface immediately above the headscarp of the lower landslide. The slump measured approximately 3 m long, 1 m high and 2.5 m wide.

Rainfall infiltration and perched water were likely sources of pore-water pressure that reduced effective stresses and shear strength. The debris from the upslope slump and the increased soil weight due to water infiltration probably increased the destabilizing forces in the slope. The ongoing hillside deformation, inferred from existing tension cracks and curved trees, indicates that the soil mobilized ultimate stress states leading up to the slope failure when the safety factor dropped to less than unity.

8 MIDDLE LANDSLIDE

The landslide initiated on the slope approximately 8 to 10 m downslope from the trail. During the site visit, the section of the trail above the landslide was moist, suggesting that seepage exits the hillside near the trail elevation. Figure 11 shows the landslide origin, inferred perched water level, and hillside geology.

The landslide made a rapid transition into a shallow debris flow. The landslide volume was roughly 75 m³. Mudlines from the debris flow were visible approximately 5 m above the base of trees located 30 to 40 m downslope from the headscarp. The mudlines and lack of debris deposited on a small 32° sloping bench suggest that the water content of the landslide materials was very high at

the time of occurrence. The fluidized debris flowed over a bedrock-controlled crest mid-way up the valley wall at an approximate elevation of 515 m before it descended rapidly to Mission Creek. This landslide had characteristics similar to the west landslide and is classified as a flowslide.

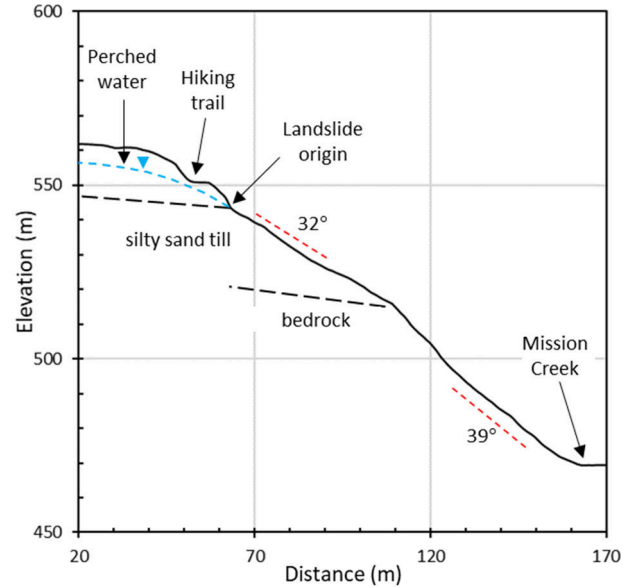


Figure 11. Slope profile for the middle landslide

For both the west and middle landslides, reduced suction due to the rainfall infiltration and hillside deformations might have contributed to the failure mechanism, and these will be explored in further studies.

9 EAST LANDSLIDE

The east landslide was the largest event and differed from the other two landslides because it was caused by overland water flow. The flowing water caused erosion and scour within two drainage channels that merged into a larger drainage gully below the trail. This event was likely associated with high runoff originating from the gullies' headwaters above the trail in an area undergoing earthworks for residential development. Field evidence indicates a transition from concentrated rapid runoff to a scouring debris flow or flood downslope from the trail. The transported sediment and debris travelled approximately 180 m from just above the trail to Mission Creek. Figure 12 shows the slope profile along the centre of the main gully and the western branch gully above the trail.

The downcutting in the main gully below the trail occurred through a thick sequence of silts and sands, causing the gully to become quite incised. Figure 13 shows cross-sections of the gully at two different elevations. Midslope, the gully measures approximately 3 to 4 m deep, roughly 8 m wide, with steep (80%) side slopes.

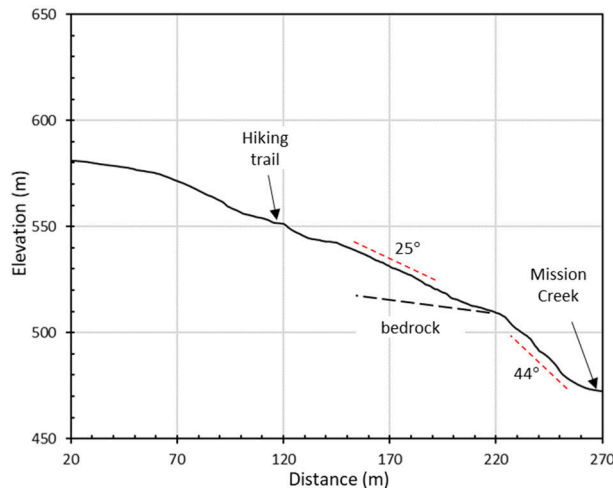


Figure 12. Slope profile for the east landslide

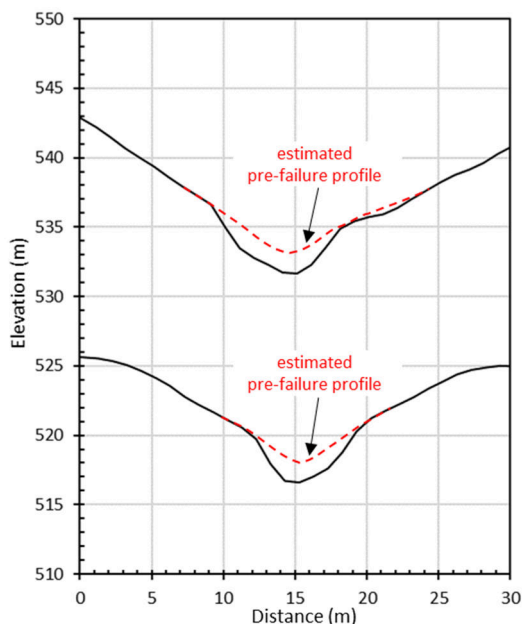


Figure 13. Two cross-sections for the east landslide

Approaching Mission Creek, the gully encounters bedrock before descending a very steep bedrock-controlled section. The debris carried down the gully was deposited on a gently sloping terrace at the edge of Mission Creek as well as into the creek. The landslide debris (soil, boulders, and woody debris) was up to 1 m thick on the terrace. The deposition area (fan) covers 300 to 350 m². Mudlines on trees in the runout zone adjacent to Mission Creek were 5 to 6 m above the ground surface, which is a testament to the event's high discharge and fluid nature. The volume of debris carried down to Mission Creek is estimated at 400 m³.

Field observations and geometrical features suggest that the landslide is classified as a debris flow or flood event according (Wilford et al. 2004).

10 CONCLUSIONS

Lidar data supplemented with SfM point cloud data generated from images taken by a drone were used to investigate three small landslides near a hiking trail along a steep valley wall. The landslides occurred in glacial sediments and were triggered by a short period of heavy rainfall in the spring. The layered nature of the glaciofluvial and glacial till soils is believed to have created perched water tables that also contributed to the west and middle landslides. The loose fill placed on the steep slope during the old cut and fill excavation for the trail might also be a contributing factor to the west and middle landslides.

REFERENCES

- Asghar, U. and Tannant, D.D. 2018. Landslide mapping from structure-from-motion analysis of photos acquired by a drone. *7th Canadian Geohazards Conference*, Canmore. 9 p.
- Historical Radar 2018. Canadian Historical Weather Radar for May 9, 2018. https://climate.weather.gc.ca/radar/index_e.html
- ClimateBC. 2021. ClimateBC_Map – A interactive platform for visualization and data access. http://www.climatewna.com/ClimateBC_Map.aspx
- Hungr, O., Evans, S.G., Bovis, M. and Hutchinson, J.N. 2001. Review of the classification of landslides of the flow type. *Environmental & Engineering Geoscience* 7(3): 221-238.
- Hungr, O., Leroueil, S. and Picarelli, L. 2014. The Varnes classification of landslide types, an update *Landslides* 11: 167–194.
- LidarBC. 2021. Open LiDAR Data Portal. <https://governmentofbc.maps.arcgis.com/apps/MapSeries/index.html?appid=d06b37979b0c4709b7fcf2a1ed458e03>
- NRC 2022. Canadian Spatial Reference System Precise Point Positioning Tool. Natural Resources Canada <https://webapp.geod.nrcan.gc.ca/geod/tools-ouils/ppp.php>
- Okulitch, A.V. (comp.) 2013. Geology, Okanagan Watershed, British Columbia, Geological Survey of Canada, Open File 6839, scale 1:100 000.
- Ruzesky, T. and Carter, J. 1990. *Paying for Rain: A History of the South East Kelowna Irrigation District*.
- Wilford, D.J., Sakals, M.E., Innes, J.L., Sidle, R.C. and Bergerud, W.A. 2004. Recognition of debris flow, debris flood and flood hazard through watershed morphometrics. *Landslides* 1(1): 61-66.